

# PCCP

Accepted Manuscript



This is an *Accepted Manuscript*, which has been through the Royal Society of Chemistry peer review process and has been accepted for publication.

*Accepted Manuscripts* are published online shortly after acceptance, before technical editing, formatting and proof reading. Using this free service, authors can make their results available to the community, in citable form, before we publish the edited article. We will replace this *Accepted Manuscript* with the edited and formatted *Advance Article* as soon as it is available.

You can find more information about *Accepted Manuscripts* in the [Information for Authors](#).

Please note that technical editing may introduce minor changes to the text and/or graphics, which may alter content. The journal's standard [Terms & Conditions](#) and the [Ethical guidelines](#) still apply. In no event shall the Royal Society of Chemistry be held responsible for any errors or omissions in this *Accepted Manuscript* or any consequences arising from the use of any information it contains.

# Improvement of Desolvation and Resilience of Alginate Binders for Si-based Anode in a Lithium Ion Battery by Calcium-Mediated Cross-linking<sup>†</sup>

Cite this: DOI: 10.1039/x0xx00000x

Jihee Yoon,<sup>#a</sup> Dongyeop X. Oh,<sup>#b</sup> Changshin Jo,<sup>#a</sup> Jinwoo Lee,<sup>\*a</sup> and Dong Soo Hwang<sup>\*b,c</sup>

Received 00th January 2012,

Accepted 00th January 2012

DOI: 10.1039/x0xx00000x

[www.rsc.org/](http://www.rsc.org/)

Si-based anodes in lithium ion batteries (LIBs) have exceptionally high theoretical capacity, but the use of a Si-based anode in LIB is problematic because the charging/discharging process can fracture the Si. Alginate and its derivatives show promise as Si particle binders in the anode. We show that calcium-mediated “Egg-box” electrostatic cross-linking of alginate improves toughness, resilience, electrolyte desolvation of the alginate binder as a Si-binder for LIBs. Consequently, the improved mechanical properties of calcium alginate binder compared to the sodium alginate binder and other commercial binders extend the lifetime and increase the capacity of Si-based anodes in LIBs.

## 1. Introduction

The need for rechargeable lithium ion batteries (LIBs) has rapidly increased because of the growing markets for smart phones and electric/hybrid vehicles.<sup>1, 2</sup> However, graphitic carbon-based anode, commonly used anode in LIBs, has low theoretical capacity (372 mA h g<sup>-1</sup>). Thus, other types of Li ion host materials have been actively investigated by many researchers.<sup>3-9</sup> Among them, Si-based anodes in lithium ion batteries (LIBs) has been suggested as an alternative due to its exceptionally high theoretical capacity (4200 mA h g<sup>-1</sup>), low cost, and natural abundance.<sup>10-14</sup>

However, the mechanical instability of Si-based anodes in LIBs has impeded their practical application.<sup>15-18</sup> Generally, the Si-based anode is a composite composed of Si particles (active material), carbon (conducting agent), and polymeric binder. During the charging/discharging process, Li ion and Si undergo alloy-de-alloy phase transition to Li<sub>4.4</sub>Si. As a consequence, the volume of Si particles more than triples; the mechanical stress caused by this expansion can crack and fracture the anode composites. This process leads to serious degradation of electrical contact between active materials and current collector.

Thus, this problem reduces the battery cycling life time and is one of the main obstacles in commercialization of Si-based anodes in LIBs.<sup>12, 18, 19</sup>

To prevent this mechanical damage to the anode composite, many studies have focused on developing a polymeric binder for the anode composite. The binder must (i) improve the adhesion strength between anode composite and current collector, (ii) retain the binding with Si during Li-charging/discharging cycling, and (iii) decrease the Li ion loss by forming stable solid electrolyte interphase (SEI) layer.<sup>16, 20, 21</sup> The physical and chemical properties of the binder have a critical effect on these abilities. To date, biopolymers such as carboxymethyl cellulose (CMC) and alginate show promise as binders.<sup>16, 20, 22</sup> Some recent studies have revealed that the self-healable polymeric binders that have the chemically incorporated ability to repair mechanical damage can contribute to high capacity and stable performance of a battery.<sup>13, 19</sup> This self-healing property of the binder can continuously repair the mechanical damages in the binders during sequential charging/discharging, and thereby extend the lifetime of Si-anode composites in LIBs.

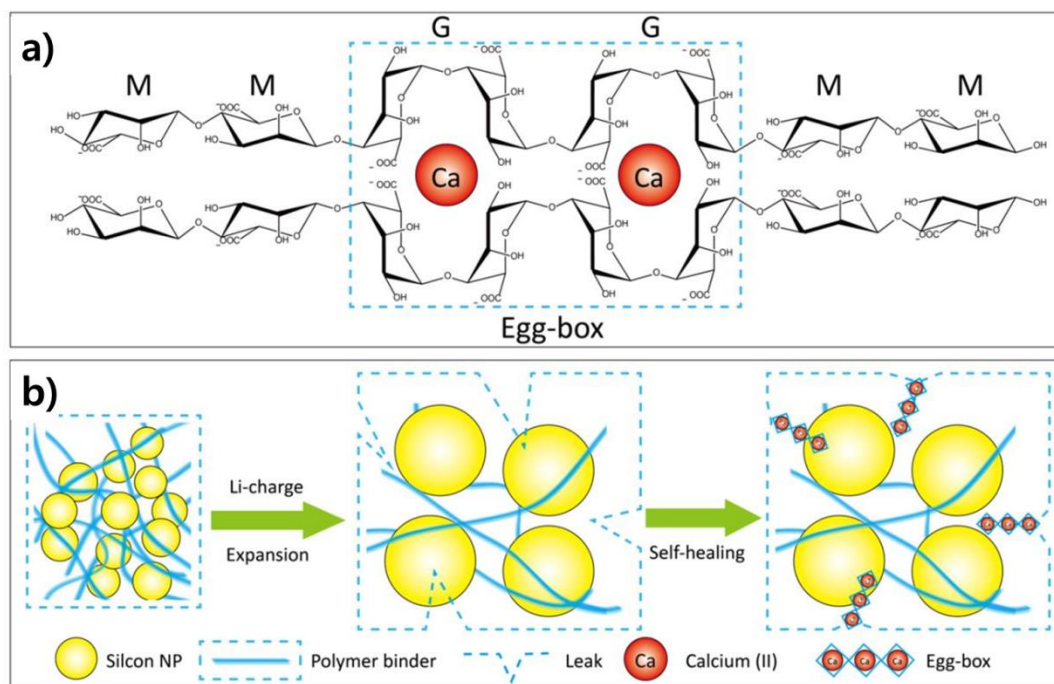


**Fig. 1** (a) Molecular structure of alginate and Ca-mediated “egg-box” like cross-links in Ca-alginate. (b) Expansion and self-healing mechanism of Ca-alginate-containing silicon anode during charge-discharge cycles.

The biochemistry of brown algal cell walls suggests in-sight to provide self-healing properties to the binders. Alginate, a copolymer of  $\beta$ -D-mannuronate units (M block) and  $\alpha$ -L-guluronate (G block) connected by 1,4 linkages (Fig. 1a), forms reversible and self-healable bonds in the presence of calcium (Ca<sup>2+</sup>) or magnesium (Mg<sup>2+</sup>) ions in the cell walls of brown algae.<sup>23, 24</sup> Alginate acquires extreme toughness and resilience in the presence of Ca<sup>2+</sup>.<sup>25</sup> G blocks of alginate selectively couple with Ca<sup>2+</sup> to form a row of reversible and strong electrostatic cross-links called “the egg-box structure” (Fig. 1b).<sup>26</sup> The high unzipping energy of the cross-links can enhance alginate’s stiffness and toughness; furthermore, re-zipping of cross-links spontaneously heals the mechanical damages to the cell wall of brown algae.<sup>25, 27, 28</sup> Very recently, it was reported that Ca<sup>2+</sup> added alginate was used as a binder for Si-anode.<sup>28</sup> However; they did not study the origin of the improved performance of Ca<sup>2+</sup> added alginate as a binder for Si-anode.

In this study, we fabricated brown Ca<sup>2+</sup>-doped-alginate (Ca-alginate) binder to achieve a Si anode composite with enhanced stiffness, toughness, and resilience compared to sodium alginate (Na-alginate), CMC, and PVDF binders due to reversible Ca-mediated cross-link. To fabricate electrode more efficiently, the simple Ca-spray treatment method was applied in this work. To prove the origin of the improved performance of cross-linked alginate by sprayed Ca<sup>2+</sup> ions as a binder for Si-anode, the improvement in the desolvation and resilience of cross-linked alginate was studied by electrolyte absorption and tensile tests. The proved improvement was well-correlated to the performance of Si-based anodes in LIBs. As a consequence, LIBs that use the Ca-alginate binder demonstrated longer life

time and higher charge capacity than those with Na-alginate, CMC, and PVDF binders.

## 2. Experimental Section

### 2.1. Materials

Si powder (APS=100 nm, 99%, Alfa Aesar) and Super P conducting carbon (TIMCAL, Switzerland) were used as active materials and conductive carbon black respectively for the Si electrode. Sodium alginate was purchased from MP Biomedical LLC, USA. CaCl<sub>2</sub>, CMC, PVDF, and EDTA (Ethylenediaminetetraacetic acid) was purchased from Sigma-Aldrich. A mixture of ethylene carbonate/ethyl methyl carbonate (EC/EMC, 3:7 volume ratio, Panaxetec Co., Korea) in 1.3M lithium hexafluorophosphate (LiPF<sub>6</sub>) was used as the electrolyte. The electrolyte also contains 10 wt% of fluoroethylene carbonate (FEC) as an additive. Polypropylene (PP) film was used as separators.

### 2.2. Film preparation

Three types of alginate films were prepared: Na-alginate, Ca-alginate, EDTA-treated Ca-alginate. Alginate powder was dissolved in 1 wt% in distilled water and cast as described previously.<sup>29</sup> Na-alginate films were prepared by drying the solutions on a glass dish at 40 °C in a convection oven overnight. Ca-alginate was prepared by immersing Na-alginate film in 1 wt% CaCl<sub>2</sub> ethanol solution for 30 min. The Ca-

alginate films were washed with ethanol and dried at room temperature (RT) for 6 h. EDTA-treated Ca-alginate was prepared by immersing the dried Ca-doped film in a 7:3 (v:v) mixture of 0.1 M EDTA and the Ca-alginate/ethanol mixture for 1 d. The resulting EDTA-treated film was washed with ethanol and dried at RT. Ethanol inhibited dissolution of alginate into water. CMC films were prepared in the same manner used to prepare the Na-alginate film. Commercial PVDF film was used as received.

### 2.3. Characterization of thermal properties and electrolyte absorption

Thermograms of the binders films were recorded at a heating rate of 10 °C/min using a differential scanning calorimeter (DSC, Perkin-Elmer).<sup>24</sup> Electrolyte absorption of the films was quantified to study swelling behavior of binders. Dry samples were weighed to an accuracy of 10<sup>-4</sup> g ( $W_{\text{before}}$ ), immersed in the electrolyte (EC/EMC) for 6 h at 30 °C to allow them to become saturated with electrolyte, then weighed ( $W_{\text{after}}$ ) again after excess electrolyte was wiped from their surfaces. Electrolyte absorption was calculated as  $\frac{W_{\text{after}} - W_{\text{before}}}{W_{\text{before}}} \times 100$ .<sup>28</sup>

### 2.4. Tensile tests

Tensile properties of the films were measured using a universal tensile tester (Instron, Norwood, UK). All films were dried for 12 h in a vacuum oven before immersion to the electrolyte. The dried films were cut into 30 mm × 5 mm rectangles, then immersed in electrolyte for 6 h at 30 °C. The immersed films were taken out, clamped onto the grips with 10 mm distance, and loaded with a constant strain rate of 0.5 mm/min until failure.<sup>29</sup> To calculate the tensile stress (load per unit cross-sectional area, MPa) on the films, the thickness of the films was determined using a micrometer before the test.

Cyclic tensile tests before fracture were performed as follow.<sup>30, 31</sup> Different loading strains (5, 10, and 20 %) and a return back to 0 % strain constituted each cycle of strain recovery experiment. Residual strain was defined as the deformed strain at which tension occurred (i.e.,  $\sigma$  abruptly increased from 0 MPa) in the next cycle. Recovered strain was calculated as  $\frac{\text{Total strain} - \text{Residual strain}}{\text{Total strain}} \times 100$ . At least three specimens of each sample were tested in this manner.

### 2.5. Electrochemical Characterization

For the preparation of electrodes, Si powder was mixed with Super P and Na-alginate binder (3:1:1, weight ratio) in deionized water. The slurry was coated on a Cu foil using the doctor-blading technique and dried at 60 °C for 1 h, and then 1 wt% CaCl<sub>2</sub> solution was sprayed on the slurry at 0.23 mL min<sup>-1</sup> (Fig. S1). The resulting electrode was dried for at least 4 h.

Then, the cast film was dried in a vacuum oven at 110 °C for at least 8 h. The mass loading of Si was 0.4–0.5 mg cm<sup>-2</sup>.<sup>20</sup>

The half-cell test was conducted with a coin-type two-electrode cell (CR2032). The lithium foil was used as both counter and reference electrodes. The unit cells were galvanostatically cycled between 0.01 and 1.0 V (vs. Li/Li<sup>+</sup>) at 200 mA g<sup>-1</sup> in the pre-cycle and thereafter cycled at 1000 mA g<sup>-1</sup> using a WBCS-3000 battery cycler (Xeno Co.). Coulombic efficiency was calculated as  $\frac{C_{\text{dealloy}}}{C_{\text{alloy}}} \times 100$ , where  $C_{\text{alloy}}$  and  $C_{\text{dealloy}}$  are the capacities of the anodes for Li insertion and extraction respectively.

## 3. Results and Discussion

### 3.1. Preparation of binder films

Five types of binders were cast as thin films to examine the effect of calcium-mediated crosslinking on the physical properties of the binder: Na-alginate, Ca-alginate, EDTA-treated Ca-alginate, CMC, and PVDF. In our anode system, the Ca ions were introduced to the alginate binder by spraying the CaCl<sub>2</sub> solution on the dried anode film, instead of directly adding the CaCl<sub>2</sub> powder into the wet anode slurry since the Ca-containing anode slurry is too viscous and heterogeneous to be processed. The uniform distribution of the calcium ions in the film after the CaCl<sub>2</sub>-spray treatment was confirmed by the element map of the cross-section of the film by Energy-dispersive X-ray spectroscopy (EDS) (Fig. S2 & S3). Likewise, Ca-alginate film was prepared by immersing the dried Na-alginate film in CaCl<sub>2</sub> solution instead of directly adding CaCl<sub>2</sub> powder into Na-alginate solution before film formation. The EDTA treatment was performed to remove Ca<sup>2+</sup> from Ca-alginate film.<sup>32</sup> CMC and PVDF are representative of bio-based polymer binder and synthetic polymer binder. We expected that the addition of Ca<sup>2+</sup> may induce electrostatic reversible and self-healable electrostatic bonds between calcium ion and carboxyl group in alginate, improve the physical properties of alginate binder for Si-anode binder, and extend the life time of the Si-anode composite with alginate. (Fig. 1)

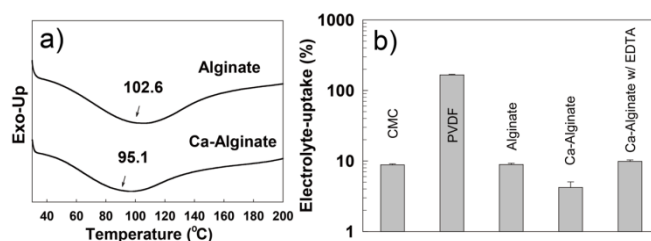
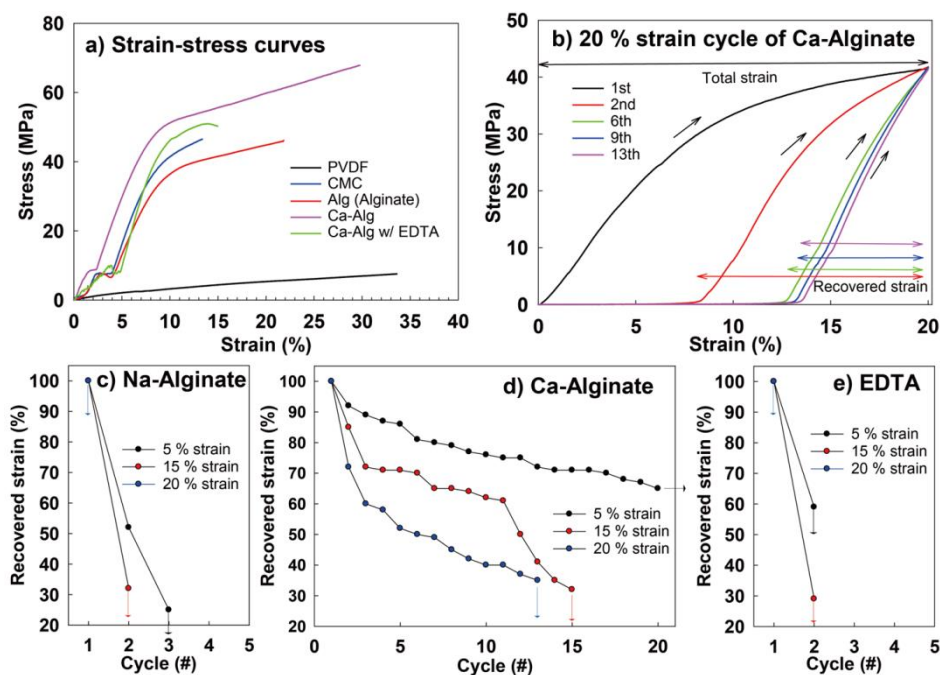


Fig. 2 (a) Thermograms and  $T_g$  values of Na-alginate and Ca-alginate (b) Electrolyte-uptake values (EC/EMC) of CMC, PVDF, Na-alginate, Ca-alginate, and EDTA-treated Ca-alginate films. Arrows:  $T_g$ .



**Fig. 3** Tensile properties of binders in the presence of the electrolyte. (a) Stress-strain curves of CMC, PVDF, Na-alginate, Ca-alginate, and EDTA-treated Ca-alginate films. (b) The cyclic tensile tests of Ca-alginate with 20% strain. The recovered strain values of (c) Na-alginate, (d) Ca-alginate, and (e) EDTA-treated Ca-alginate during cyclic tensile tests with different loading strain (down-arrow means fracture).

### 3.2. Thermodynamic evidence for Ca-mediated cross-links in alginate

To investigate whether immersion of dried Na-alginate in  $\text{CaCl}_2$  solution could induce Ca-mediated cross-links, glass transition temperature ( $T_g$ ) values of Ca-alginate and Na-alginate (Fig. 2a) were measured because  $T_g$  change is thermodynamically correlated with the degree of cross-linking in a polymer.<sup>24, 26, 33</sup> Ca-mediated cross-links of alginate is known to decrease the  $T_g$  of alginate because the insertion of Ca ion with larger radius than Na ions into G blocks of alginate increases its free volume.<sup>24, 26, 33</sup> Ca-alginate films showed lower  $T_g$  ( $\sim 95.1$  °C) than did Na-alginate ( $\sim 102.6$  °C); this difference implies that the  $\text{Ca}^{2+}$  introduced into the anode by absorption of  $\text{CaCl}_2$  solution formed Ca-mediated cross-links of alginate binder, as does direct addition of  $\text{CaCl}_2$  powder to alginate aqueous solution.<sup>14, 16, 22</sup>

### 3.3. Effect of calcium addition on the electrolyte-desolvation, mechanical properties, and resilience of alginate

Electrolyte solvation of polymeric binders reduces molecular interaction strengths between binders or between binder and Si particles.<sup>16, 20, 34, 35</sup> Thus, electrolyte over-uptake of the binder can eventually degrade the battery performance due to softening of the binder and weak adhesion between the binder and the Si particle. Thus, we measured the electrolyte

adsorption values of the binder films (Fig. 2b). Electrolyte absorption values of the alginate films regardless of  $\text{Ca}^{2+}$  addition were much lower than that of PVDF ( $\sim 165$  %). Ca-alginate showed lower electrolyte uptake ( $\sim 4.2$  %) than did Na-alginate ( $\sim 8.7$  %).<sup>36</sup>  $\text{Ca}^{2+}$  was removed from the Ca-alginate film by EDTA and the electrolyte-uptake of the Ca-alginate film rose to  $\sim 9.0$  %, which is comparable to Na-alginate. Presumably, the G-unit segments of alginate in the presence of calcium ions are likely to form “egg-box” like cross-links that prevent electrolyte from infiltrating the film (Fig. 1).<sup>26, 36</sup> The electrolyte absorption of PVDF ( $\sim 165$  %) was much higher than those of the other biopolymer binders, and that of CMC ( $\sim 8.8$  %) was as low as that of Na-alginate. The results are likely due to the fact that PVDF is an organo-soluble polymer whereas Na-alginate and CMC are water-soluble polymers.

To guarantee extended life time of a binder that is subjected to continual mechanical stresses during the Li-charging/discharging process, mechanical properties of binder polymers in the presence of the electrolyte medium should be improved. The low electrolyte (solvent) uptake of the Ca-alginate films was expected to suppress softening of Ca-alginate due to electrolyte solvation, and the reversible and strong Ca-mediated cross-links were expected to improve stiffness, toughness, and resilience of the electrolyte-absorbed alginate. Therefore, tensile properties of electrolyte-absorbed Na-alginate were compared to those of electrolyte-absorbed Ca-alginate (Fig. 3a).<sup>37, 38</sup>

In the presence of the electrolyte, the Ca-alginate had stiffness of  $510 \pm 21$  MPa and toughness of  $13.5 \pm 3.1$  MJ $\cdot\text{m}^{-3}$ ; these values are much higher than those of Na-alginate:

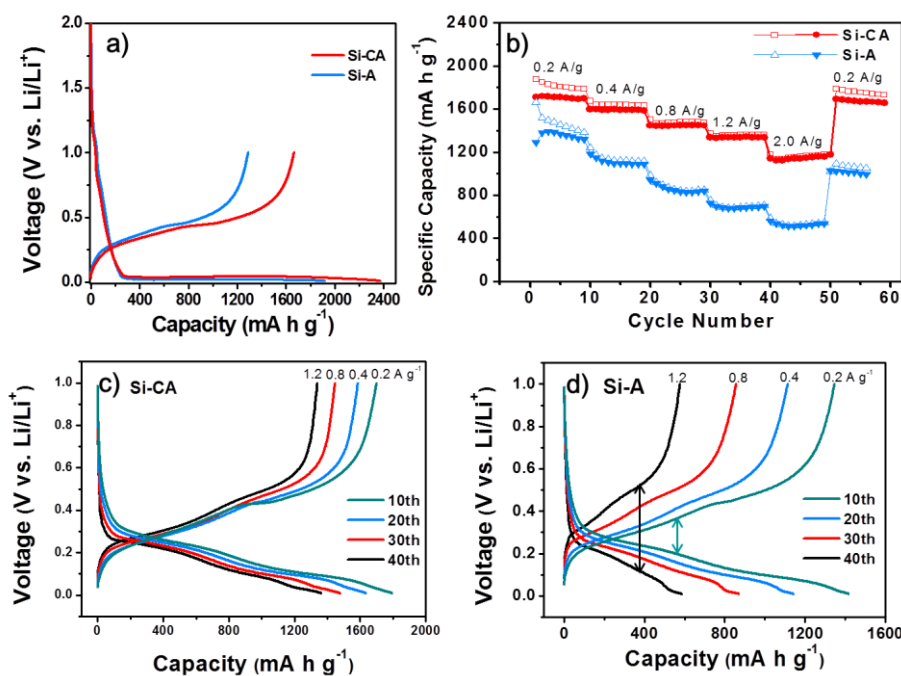


**Fig. 4** (a) Charge-discharge profiles of Si-CA and Si-A during pre-cycling. The electrodes were measured at 200 mA g<sup>-1</sup> in the range of 0.01–1.0 V (versus Li/Li<sup>+</sup>). (b) Rate performance plots of Si-CA and Si-A. Charge-discharge profiles of (c) Si-CA and (d) Si-A obtained at various current densities, 0.2 to 1.2 A g<sup>-1</sup>. Arrows indicate voltage gaps between charge-discharge curves.

stiffness of  $121 \pm 6$  MPa and toughness of  $4.8 \pm 0.5$  MJ·m<sup>-3</sup>. After EDTA treatment, the tensile properties of the electrolyte-absorbed Ca-alginate decreased to stiffness of  $132 \pm 12$  MPa and toughness of  $3.3 \pm 0.6$  MJ·m<sup>-3</sup>, which are similar to those of Na-alginate. These results suggest that addition of Ca<sup>2+</sup> to alginate film caused the tensile properties of the Ca-alginate film to be superior to those of the Na-alginate film. Tensile properties of the electrolyte-absorbed Ca-alginate were also superior to those of commercial binders (PVDF:  $32 \pm 2$  MPa stiffness,  $1.2 \pm 0.1$  MJ·m<sup>-3</sup> toughness, CMC:  $112 \pm 19$  MPa stiffness,  $2.8 \pm 0.1$  MJ·m<sup>-3</sup> toughness). Probably, the improved tensile properties of Ca-alginate compared to the others can be attributed to the high un-zipping energy of the egg-box structure.<sup>25</sup>

The resilience of a binder, represents its ability to return to its original state after cyclic mechanical stress, and is also an important mechanical parameter.<sup>39, 40</sup> Strain recovery of electrolyte-solvated Ca-alginate, Na-alginate, and EDTA-treated Ca-alginate were monitored during cyclic tensile tests with different loading strain (5, 10, and 20 %) (Fig. 3b-e). Since the volume of Si particles in the battery expands by more than triple with the full Li charging, ~15% of the loading strain would be the maximum loading strain in the practical Li-battery during charging.

At 5% loading strain, the strain recovery of Ca-alginate decreased gradually to ~65 % at the 20th cycle but the film did not break even after 20 cycles. In the same condition, the strain recovery of Na-alginate film decreased rapidly and the film broke after at most three cycles. At both 10 % and 20 % of

loading strain, the strain recovery of Ca-alginate decreased more than that of Na-alginate which broke after most two cycles. To further understand the effect of Ca<sup>2+</sup> on resilience of alginate, the same tensile tests were performed on the EDTA treated Ca-alginate film. After EDTA treatment, the resilience of the Ca-doped alginate declined to the level of the Na-alginate. These results also support the hypothesis that the Ca-alginate complex improved the resilience of alginate by spontaneously healing of internal damage by re-zipping of the egg-box structure.<sup>25</sup>

### 3.4. Electrochemical Performance

The effect of the Ca addition to the alginate binder on the Li ion battery performance was investigated in a series of galvanostatic measurements using a Si/Li two-electrode coin-cell system. Initially, the charge-discharge test was conducted in the potential range of 0.01 to 1.0 V, and the cells were cycled at 200 mA g<sup>-1</sup> for two cycles, then were tested at 1000 mA g<sup>-1</sup> in subsequent cycles. Hereafter, the Si anodes with Ca-alginate (denoted by Si-CA), alginate (Si-A), CMC (Si-C) and PVDF (Si-P) were examined in more detail, respectively.

The Ca ion improved the charge/discharge capacities of the electrodes. In the first cycle (200 mA g<sup>-1</sup>), the Si-CA electrode obtained 2370 mA h g<sup>-1</sup> lithiation (discharge) capacity and 1670 mA h g<sup>-1</sup> delithiation (charge) capacity, corresponding to 70.5 % of initial Coulombic efficiency (ICE, Charge-discharge curves in Fig. 4a). In contrast, the Si-A electrode had relatively low

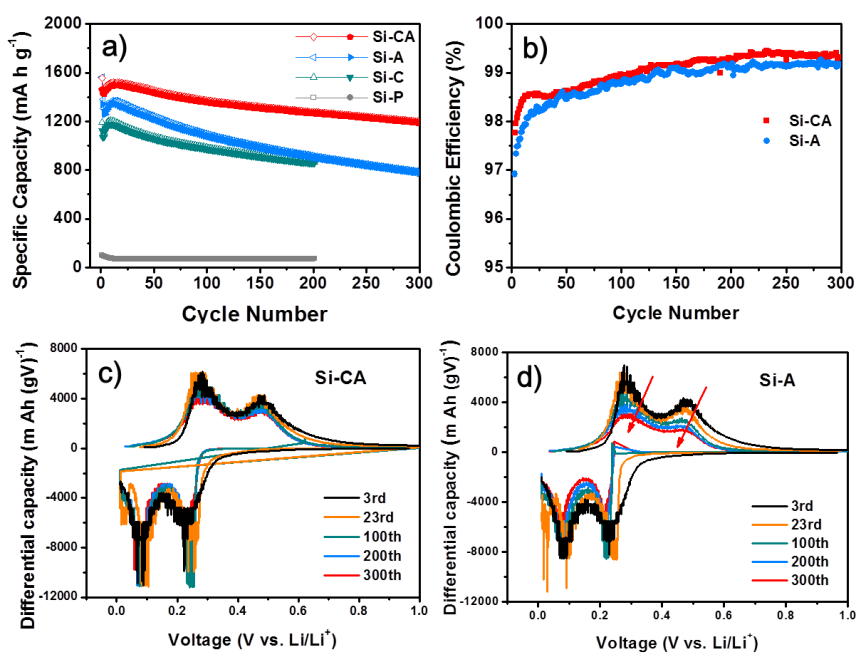


Fig. 5 Electrochemical performance of Ca-alginate binder for Si-based anode. (a) Charge capacity and (b) Coulombic efficiency of Si-based anodes with Ca-alginate (Si-CA), alginate (Si-A), CMC (Si-C), and PVDF (Si-P) at 1.0 A g<sup>-1</sup>. (c), (d) Differential capacity (dQ/dV) plots of Si-CA and Si-A.

ICEs or charge/discharge capacities. In Si-A electrode case, ICE value was 67.2 % (1920 and 1290 mA h g<sup>-1</sup> of discharge and charge capacities).

The effects of the Ca-alginate binder were verified in a rate performance test under different current densities (0.2 to 2.0 A g<sup>-1</sup>, Fig. 4b). The Si-CA electrode achieved 1711 mA h g<sup>-1</sup> charge capacity at 0.2 A g<sup>-1</sup>, and even at high current density (2000 mA g<sup>-1</sup>), 1029 mA h g<sup>-1</sup> charge capacity was obtained. This Si-CA maintained its initial high charge capacity (99 % of charge capacity retention) after 50 cycles at 200 mA g<sup>-1</sup>. In contrast, the charge capacity of Si-A gradually declined and showed 79 % retention of first charge capacity after 50 cycles at 200 mA g<sup>-1</sup>. Figure 4c and d show the charge-discharge curves of Si-CA and Si-A electrodes at different current densities. Interestingly, voltage gap of Si-A electrode increased as charging rate increase. The larger voltage gap between charge-discharge curves means that the internal resistance of Si-A electrode become larger, in which causes the capacity fading at fast charging condition. On the contrary, the Si-CA electrode exhibited small change in voltage gap even under high current density of 1.2 A g<sup>-1</sup>. In addition, with rate performance test, we found that the Ca-mediated process could decrease the internal resistance and enhance the rate performance of Si anodes.

A cycle performance was test conducted after two pre-cycles at 200 mA g<sup>-1</sup> (Fig. 5a). At 1000 mA g<sup>-1</sup>, the charge capacity was 1500 mA h g<sup>-1</sup> in the Si-CA electrode, 1360 mA h g<sup>-1</sup> in the Si-A electrode. This charge capacity of Si-CA electrode is five times higher than theoretical capacity of graphite and it was

also superior to 1170 mA h g<sup>-1</sup> in the Si-C electrode and 80 mA h g<sup>-1</sup> in the Si-P electrode.

The Si-CA electrode also showed superb cycling stability (83 % discharge capacity retention at the 300th cycle). (Capacity retention plots, Fig. S4); this value was higher than those of the other electrodes. In contrast, the charge capacity of Si-A electrode decreased drastically after the 50th cycle. The Si-A cell retained 81 %, 68 % and 58 % of the initial charge capacity at the 100, 200 and 300th cycles, respectively. In Si-C electrode, the charge capacity also declined, and was only 78 % of charge capacity retention after the 200th cycle. The charge retention of Si-P was negligible. The loading amount of Si in the anode can impact the performance of the battery. Therefore, the effect of increased Si amount on the Li ion battery performance was investigated. When the Si mass loading was increased by two folds (0.8-0.9 mg cm<sup>-2</sup>), the charge capacity (~1500 mA h g<sup>-1</sup>) was similar with that of the low Si mass loading (0.4-0.5 mg cm<sup>-2</sup>, figure S6). Moreover, with high Si mass loading, the addition of Ca to the alginate binder slowed down the charge capacity reduction.

To determine the reasons for decrease in capacity, differential capacity (dQ/dV) plots were obtained for the Si-CA electrode (Fig. 5c) and the Si-A electrode (Fig. 5d). At the 3rd cycle, both electrodes exhibited two pairs of redox peaks, which indicate two different Li<sup>+</sup> insertion/extraction processes inside the Si electrode.<sup>41, 42</sup> For Si-CA anode, the cathodic and anodic peaks were well maintained during 300 cycles; this means that, the Li<sup>+</sup> insertion and extraction reactions were highly reversible. However, in the Si-A electrode, the intensity of both cathodic and anodic peaks decreased rapidly, possibly

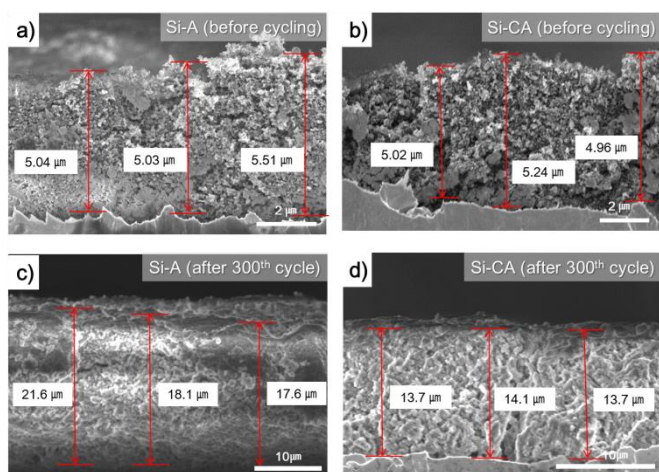


**Fig. 7** SEM images of Si-based anodes with alginate and Ca-alginate. Thickness of Si-A (a) and Si-CA (b) before cycling, and thickness of Si-A (c) and Si-CA (d) after 300th cycle.

due to structural damage to the Si electrode during repetitive charge-discharge processes. Because the Si-CA electrode was fabricated by spraying Ca-solution onto the Si-A electrode, we can infer that the added Ca-ions contributed to the improved cycle performance.

In a practical point of view, the low CE value of Si-based electrodes is another issue to be solved for the commercial use. CE values were plotted versus cycle number plots for Si-CA and Si-A electrodes (Fig. 5b). The graph corresponds to the cycle data in Fig. 5a. All CE values increased with the number of cycles, especially in the Si-CA electrode. On average, CE was 0.3-0.5 % higher in the Si-CA electrode than in the Si-A electrode. These results further confirm that the Ca-spray method can improve both the cycle-life and the reversibility of the Si electrode.

To check the thermal stability, we conducted the cycle performance test at a higher temperature (50 °C) (Figure S7). Except for the operating temperature, the other experimental conditions were the same. Even in the higher temperature cell test, Si-CA showed higher capacity and stable performance compared to Si-A. These results indicate that the Ca addition to the alginate allows high temperature tolerance; hence, the Si-CA has better thermal stability than Si-A.

Based on experimental results and this discussion, a mechanism by which electrostatic cross-links of the Ca-alginate binder contribute to the high capacity and stable cycling life time of LIBs can be proposed. First, Ca-alginate binder reduces electrolyte-uptake, which means that the interaction between binder and electrolyte is weak. Generally, a binder that uptakes excessive electrolyte, may not provide sufficient binding with Si particles and lead to relatively rapid degradation of Si.<sup>43</sup> Therefore, the low electrolyte uptake of the Ca-alginate binder (Fig. 2) prevents Si particles from decomposing during the cycling test by retaining the binder's adhesion to Si particles in the anode.

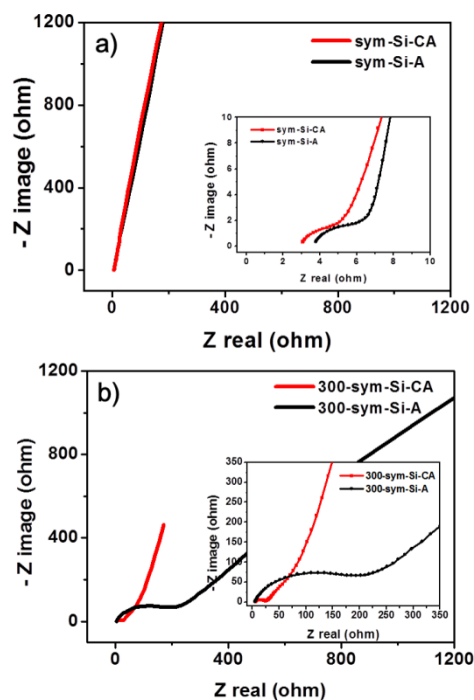


**Fig. 6** Electrochemical impedance spectroscopy (EIS) of Si-CA and Si-A (a) before cycling and (b) after 300th cycle using a Si/Si symmetric cell (SC).

Second, the unique molecular structure and chemistry of alginate may account for the excellent performance as a binder for electrodes in an LIB. Alginate is a copolymer that consists of M block and G block monomers with carboxylic acid functional groups. The carboxyl groups of alginate may form hydrogen bonds with the SiO<sub>2</sub> of the Si surface; a row of G blocks in alginate has a regular helical structure that enhances interactions between binders.<sup>16</sup> Although CMC also has carboxylic acid groups, its molecular conformation is a random coil.<sup>44</sup> We demonstrated that the electrostatic bonds between Ca-ion and alginate provide high toughness and resilience that arises from repeated zipping and unzipping of the Ca-mediated egg-box structure. Consequently, the enhanced extensibility, toughness, and resilience of Ca-alginate (Fig. 3) may help to prevent disintegration of cracked Si particles, thereby reducing Si degradation caused by the large change in the volume of Si particles during cycling.

To further confirm the effect of the Ca-alginate binder, the thickness of each Si electrode was examined in *ex-situ* scanning electron microscopy (SEM) studies.<sup>17</sup> We disassembled each Si electrode after 300 cycles. The thickness of the Si-CA electrode had increased by 2.7 times, whereas that of the Si-A electrode had increased by 3.5 times (Fig. 6). These results suggest that the electrostatic crosslinking of Ca-alginate can accommodate volume change of Si and retain cracked Si effectively.

Third, we inferred Ca-alginate binder may allow formation of a relatively stable and deformable SEI. The high CE indicates reversibility of the electrode, and stable SEI

formation.<sup>20</sup> Earlier research on alginate binder suggested that the alginate binder contributes to building a stable SEI layer on the Si surface.<sup>20</sup> We further improved the SEI layer by making electrostatic cross links between Ca and Alginate. The Si-CA electrode had higher average CE than did the Si-A electrode (Fig. 5b). The high CE of the Si-CA electrode suggests that the Ca-alginate binder helped to retain the anode composite during the cycles, and thereby minimized Li ion loss on the electrode surface and prevented collapse of Si electrode. In contrast, the Si-A electrode suffered from repeated significant volume change, which fractures Si particle, so the Si fragmented to form an additional SEI layer.

To further investigate the performance of the anodes, we conducted electrochemical impedance spectroscopy (EIS) measurements using a Si/Si symmetric cell (SC) configuration.<sup>45, 46</sup> We chose the SC system to exclude the signal from the Li metal. The electrodes before and after cycling (300th charge) were cut in half and assembled inside a glove box. The Nyquist plots of all SCs showed typical graph, composed of a semicircle at high frequency and a sloped line at low frequency. The semicircle represents charge-transfer between electrode and electrolyte, and the sloped line is related to the Warburg diffusion process into the electrode. The Nyquist plots of pristine Si-CA and Si-A SCs were similar in size and shape (Fig. 7a), but those of SCs fabricated from electrodes that had been cycled exhibited great differences in shape (Fig. 7b). The sizes of semicircles increased in both SCs but were much more severe in the Si-A SC. The Warburg diffusion term was much larger in the Si-A SC than in the Si-CA SC. The EIS results suggest that the internal resistance of Si-A had become serious during repetitive cycling. The volume change in Si particles results in weakened contact between Si and electrode. However, the electrochemical performance of Si-CA electrode implies that the calcium spray process results improved the Si electrode by contributing additional cross-linking between binders.

#### 4. Conclusions

Ca-alginate binder demonstrated promising mechanical properties due to Ca-mediated “egg-box” like electrostatic cross links enable a silicon anode to endure catastrophic volume change. High unzipping energy, spontaneous re-zipping, and electrolyte-desolvation of the cross-links provided significant improvement in stiffness, toughness, and resilience of the electrolyte-solvated alginate binder compared to Na-alginate and other commercial binders. Consequently, the improved mechanical properties of Ca-doped alginate extend the lifetime and increase the capacity of Si-based-anode LIB. This strategy implies further improvement of the alginate as a silicon anode binder of LIB is possible by new chemistry and engineering.

#### Acknowledgements

We acknowledge Marine Biotechnology Program funded by the Ministry of Oceans and Fisheries, Korea, and the National Research Foundation of Korea Grants funded by the Korean Government (MEST) (NRF-C1ABA001-2011-0029960, NRF-2012R1A2A2A01002879, and NRF-2013-Fostering Core Leaders of the Future Basic Science Program). This work was further supported by a grant of the Korea Health 21 R&D Project of Ministry of Health & Welfare (A121631)

#### Notes and references

<sup>a</sup> Department of Chemical Engineering, Pohang University of Science and Technology (POSTECH), Pohang, 790-784, Republic of Korea. Email: jinwoo03@postech.ac.kr

<sup>b</sup> Ocean Science and Technology Institute, Pohang University of Science and Technology (POSTECH), Pohang, 790-784, Republic of Korea.

<sup>c</sup> School of Environmental Science and Engineering and Division of Interdisciplinary Bioscience and Bioengineering, Pohang University of Science and Technology (POSTECH), Pohang, 790-784, Republic of Korea. Email: dshwang@postech.ac.kr

† Electronic Supplementary Information (ESI) available: Additional data and pictures. See DOI: 10.1039/b000000x/

# These authors contributed equally to this work.

1. A. S. Aricò, P. Bruce, B. Scrosati, J.-M. Tarascon and W. Van Schalkwijk, *Nat. Mater.*, 2005, 4, 366-377.
2. N. S. Choi, Z. Chen, S. A. Freunberger, X. Ji, Y. K. Sun, K. Amine, G. Yushin, L. F. Nazar, J. Cho and P. G. Bruce, *Angew. Chem. Int. Edit.*, 2012, 51, 9994-10024.
3. J. Jiang, Y. Li, J. Liu, X. Huang, C. Yuan and X. W. D. Lou, *Adv. Mater.*, 2012, 24, 5166-5180.
4. J. Hwang, S. H. Woo, J. Shim, C. Jo, K. T. Lee and J. Lee, *ACS nano*, 2013, 7, 1036-1044.
5. C. Jo, Y. Kim, J. Hwang, J. Shim, J. Chun and J. Lee, *Chem. Mater.*, 2014, 26, 3508-3514.
6. S. Yoon, C. Jo, S. Y. Noh, C. W. Lee, J. H. Song and J. Lee, *Phys. Chem. Chem. Phys.*, 2011, 13, 11060-11066.
7. E. Kang, Y. S. Jung, G. H. Kim, J. Chun, U. Wiesner, A. C. Dillon, J. K. Kim and J. Lee, *Adv. Funct. Mater.*, 2011, 21, 4349-4357.
8. F.-W. Yuan and H.-Y. Tuan, *Chem. Mater.*, 2014, 26, 2172-2179.
9. V. G. Pol and M. M. Thackeray, *Energy Environ. Sci.*, 2011, 4, 1904-1912.
10. J.-K. Yoo, J. Kim, Y. S. Jung and K. Kang, *Adv. Mater.*, 2012, 24, 5452-5456.
11. T. D. Bogart, D. Oka, X. Lu, M. Gu, C. Wang and B. A. Korgel, *ACS Nano*, 2013, 8, 915-922.
12. B. Koo, H. Kim, Y. Cho, K. T. Lee, N. S. Choi and J. Cho, *Angew. Chem. Int. Edit.*, 2012, 51, 8762-8767.
13. Y. K. Jeong, T. W. Kwon, I. Lee, T. S. Kim, A. Coskun and J. W. Choi, *Nano Lett.*, 2014, 14, 864-870.
14. R. Yi, F. Dai, M. L. Gordin, S. Chen and D. Wang, *Adv. Energy. Mater.*, 2013, 3, 295-300.
15. H. Wu, G. Yu, L. Pan, N. Liu, M. T. McDowell, Z. Bao and Y. Cui, *Nat. Comm.*, 2013, 4,

16. A. Magasinski, B. Zdyrko, I. Kovalenko, B. Hertzberg, R. Burtovyy, C. F. Huebner, T. F. Fuller, I. Luzinov and G. Yushin, *ACS Appl. Mater. Interfaces.*, 2010, 2, 3004-3010.
17. Y. Park, S. Lee, S.-H. Kim, B. Y. Jang, J. S. Kim, S. M. Oh, J.-Y. Kim, N.-S. Choi, K. T. Lee and B.-S. Kim, *RSC Adv.*, 2013, 3, 12625-12630.
18. N. Liu, H. Wu, M. T. McDowell, Y. Yao, C. Wang and Y. Cui, *Nano Lett.*, 2012, 12, 3315-3321.
19. C. Wang, H. Wu, Z. Chen, M. T. McDowell, Y. Cui and Z. Bao, *Nat. Chem.*, 2013, 5, 1042-1048.
20. I. Kovalenko, B. Zdyrko, A. Magasinski, B. Hertzberg, Z. Milicev, R. Burtovyy, I. Luzinov and G. Yushin, *Science*, 2011, 334, 75-79.
21. J. Song, M. Zhou, R. Yi, T. Xu, M. L. Gordin, D. Tang, Z. Yu, M. Regula and D. Wang, *Adv. Funct. Mater.*, 2014.
22. J. S. Bridel, T. Azaïs, M. Morcrette, J. M. Tarascon and D. Larcher, *Chem. Mater.*, 2009, 22, 1229-1241.
23. O. Smidsrød and G. Skjåk-Bræk, *Trends. Biotechnol.*, 1990, 8, 71-78.
24. R. Russo, M. Malinconico and G. Santagata, *Biomacromolecules*, 2007, 8, 3193-3197.
25. J. Y. Sun, X. Zhao, W. R. K. Illeperuma, O. Chaudhuri, K. H. Oh, D. J. Mooney, J. J. Vlassak and Z. Suo, *Nature*, 2012, 489, 133-136.
26. L. Li, Y. Fang, R. Vreeker, I. Appelqvist and E. Mendes, *Biomacromolecules*, 2007, 8, 464-468.
27. T. Baumberger and O. Ronsin, *Biomacromolecules*, 2010, 11, 1571-1578.
28. J. Liu, Q. Zhang, Z.-Y. Wu, J.-H. Wu, J.-T. Li, L. Huang and S.-G. Sun, *Chem. Commun.*, 2014, 50, 6386-6389.
29. D. X. Oh and D. S. Hwang, *Biotechnol. Prog.*, 2013, 29, 505-512.
30. T. L. Sun, T. Kurokawa, S. Kuroda, A. B. Ihsan, T. Akasaki, K. Sato, M. A. Haque, T. Nakajima and J. P. Gong, *Nat. Mater.*, 2013, 12, 932-937.
31. C. G. Alfonso, G. Fleury, K. A. Chaffin and F. S. Bates, *Macromolecules*, 2010, 43, 5295-5305.
32. M. J. Harrington, A. Masic, N. Holten-Andersen, J. H. Waite and P. Fratzl, *Science*, 2010, 328, 216-220.
33. Ramanathan T, A. A. Abdala, Stankovich S, D. A. Dikin, M. Herrera Alonso, R. D. Piner, D. H. Adamson, H. C. Schniepp, Chen X, R. S. Ruoff, S. T. Nguyen, I. A. Aksay, R. K. Prud'Homme and L. C. Brinson, *Nat Nano*, 2008, 3, 327-331.
34. M. M. Browne, M. Forsyth and A. A. Goodwin, *Polymer*, 1997, 38, 1285-1290.
35. P. H. Mutin and J. M. Guenet, *Macromolecules*, 1989, 22, 843-848.
36. M. Davidovich-Pinhas and H. Bianco-Peled, *Carbohydrate Polymers*, 2010, 79, 1020-1027.
37. J.-W. Rhim, *LWT-Food Sci. Technol.*, 2004, 37, 323-330.
38. M. Maizura, A. Fazilah, M. Norziah and A. Karim, *J. Food Sci.*, 2007, 72, C324-C330.
39. C. M. Elvin, A. G. Carr, M. G. Huson, J. M. Maxwell, R. D. Pearson, T. Vuocolo, N. E. Liyou, D. C. Wong, D. J. Merritt and N. E. Dixon, *Nature*, 2005, 437, 999-1002.
40. S. Keten, Z. Xu, B. Ihle and M. J. Buehler, *Nat. Mater.*, 2010, 9, 359-367.
41. S.-L. Chou, J.-Z. Wang, M. Choucair, H.-K. Liu, J. A. Stride and S.-X. Dou, *Electrochem. Commun.*, 2010, 12, 303-306.
42. N. Liu, K. Huo, M. T. McDowell, J. Zhao and Y. Cui, *Sci. Rep.*, 2013, 3.
43. H.-K. Park, B.-S. Kong and E.-S. Oh, *Electrochem. Commun.*, 2011, 13, 1051-1053.
44. C. Hoogendam, A. De Keizer, M. Cohen Stuart, B. Bijsterbosch, J. Smit, J. Van Dijk, P. Van der Horst and J. Batelaan, *Macromolecules*, 1998, 31, 6297-6309.
45. E. Kang, Y. S. Jung, A. S. Cavanagh, G.-H. Kim, S. M. George, A. C. Dillon, J. K. Kim and J. Lee, *Adv. Funct. Mater.*, 2011, 21, 2430-2438.
46. G. Kim, C. Jo, W. Kim, J. Chun, S. Yoon, J. Lee and W. Choi, *Energy Environ. Sci.*, 2013, 6, 2932-2938.